Lattice dynamics of substitutional ^{119m}Sn in silicon, germanium, and α-tin using an adiabatic bond-charge model

O. H. Nielsen
Institute of Physics, University of Aarhus, DK-8000 Aarhus C, Denmark
(Received 19 January 1981)

A theoretical study of the vibrations of a substitutional impurity atom in a host lattice has been performed. The Green's-function method is treated with the purpose of enabling numerical calculations of impurity Green's functions. We consider specifically the host materials silicon, germanium, and α-tin, where the phonon dispersion curves are well described by Weber's adiabatic bond-charge model. The concepts of this model are applied to the impurity-host interactions. Numerical calculations are performed for the vibrational amplitudes of the isovalent ^{119m}Sn Mössbauer impurity in the hosts. Comparison with the recent experiments of Petersen *et al.* shows about 25% force-constant weakenings for ^{119}Sn in silicon and germanium. Localized mode frequencies for C in silicon and Si in germanium show only 4% force-constant changes.

I. INTRODUCTION

The theory of lattice dynamics for perfect crystalline materials has in the last two decades reached a high degree of sophistication, through the development of a number of phonon models which describe many physical properties. In consequence, progress has also been achieved on the lattice dynamics of isolated impurities embedded in host materials. The formalism of this problem is well known, employing the Green's-function method described by, e.g., Maradudin *et al.*[1] Both local changes of masses and force constants can be taken into account in this framework. However, the number of impurity vibration models in the literature is not so large, and the models only rarely reach the level of the best corresponding models for the perfect lattice phonons. The reason for the limited theoretical effort may be found in the fact that the impurity vibrations represent very localized and microscopic properties which are difficult to measure. A widely applied experimental technique is Mössbauer spectroscopy, where both the *s*-electron density at the impurity nucleus, as well as its amplitude of thermal vibration can be determined. The latter quantity can be compared with lattice-dynamics models, but this is not often performed, since reliable and systematic Mössbauer measurements are scarce. A review of measurements on metal hosts was given by Grow *et al.*[2] Another technique is infrared or Raman determination of localized mode frequencies for light impurities. Impurity vibrations may also play a role in the understanding of certain channeling and STAX (standing-wave x rays) experiments.

The present paper concerns the theoretical description of the vibrations of substitutional impurities. Current models relevant for the interpretation of Mössbauer data were reviewed by Grow *et al.*[2] and Petersen *et al.*,[3] and a hierarchy of models was found. (1) An impurity usually has a mass different from that of the host lattice atoms, and in this case the simple isotopic mass-defect model[4,5] predicts the gross features of the impurity vibrations. Specifically, the impurity is predicted to have, at high temperatures, the same vibrational amplitude as the host atom that it replaces. By Mössbauer experiments deviations from this simple model are usually found,[2,3] and methods are therefore needed to understand quantitatively the changes of force constants around an impurity.

(2) Only one model gives an analytical description including the effects of force-constant variation, namely, the model of Mannheim and coworkers.[6] The model was recently reformulated by Dederichs and Zeller,[7] and extended to the diamond structure.[3] It yields a very simple relation for the high-temperature ratio of the impurity-to-host vibrational amplitudes. The only parameter is the ratio of impurity-to-host force constants.[2] It was pointed out in Ref. 3, that the Mannheim model for semiconductors is oversimplified, and that the physical conclusions drawn from it are ambiguous.

(3) Therefore more sophisticated treatments based on the concepts of the perfect lattice phonon models should be considered for the impurity problem.

Phonon models for semiconductor crystals are rather complex, often employing massless pseudoparticles (shells, bond charges) to simulate the ion-ion forces transmitted by the electron cloud.[8–11] The models involve a large number of parameters (~ 10) whose physical interpretation is somewhat doubtful, and the numerical effort is substantial.[12,13] Therefore, realistic models of impurity vibrations must necessarily be complicated. Models have been constructed to describe U centers[14] and localized modes[15] in semiconductors, but the only calculation of vibrational amplitudes so far was performed by Lehman and DeWames[16] for the ^{57}Fe Mössbauer impurity in aluminum. They introduced the important concept of the *impurity dynamic response function,* which is the impurity equivalent of the phonon density of states.

In the present work the impurity vibration formalism is developed to the stage where it can be implemented for numerical calculations, and the necessary Green's functions are indicated. The amplitude of thermal vibration is also treated. The method is applied to the isovalent impurities in the group-IV semiconductors silicon, germanium, and α-tin, and in particular to the ^{119m}Sn Mössbauer impurity.[3] A realistic model of the host lattice phonons has to be selected, and its concepts applied to the impurity-host systems. The available models are summarized in the "phonon atlas" of Bilz and Kress.[17] In this work the adiabatic bond-charge model (BCM) of Weber[10,11] was chosen. It gives a particularly accurate description of the flat TA-phonon branches of the group-IV semiconductors, using only four parameters. These low-frequency phonons dominate the vibrational amplitudes, which are of particular importance in this work. It is also hoped that the BCM is more physically realistic than, e.g., an 11-parameter shell model.[18]

The paper is organized as follows: Section II describes Green's functions for models employing massless pseudoparticles. A general framework for calculation of the impurity dynamic response function is presented, and Sec. II is concluded with comments on impurity vibrational amplitudes, which are the quantities of interest in a Mössbauer experiment. In Sec. III parameter correlations of the BCM are investigated, and a reduction to only three parameters is presented. Section IV comments on the previously applied[3] Mannheim impurity model, and in Sec. V a model of an impurity within the BCM picture is presented. Numerical results for ^{119m}Sn in silicon and germanium are shown. In the appendices the relevant Kramers-Krönig relations are shown, and formulas for correlation functions are given. Methods of numerical calculations of Green's functions are discussed, and the analysis of parameter correlations is described.

II. THEORY OF IMPURITY VIBRATIONS

A. Green's functions for massless pseudoparticles

Several phonon models for semiconductors employ massless pseudoparticles, e.g., the electronlike shells of the shell model or the bond charges of the bond-charge models. These particles express the ion-ion interactions transmitted by the electron cloud. The vibrational Hamiltonian is given within the harmonic approximation by

$$H=\sum_{\alpha\ell\kappa}\frac{p_\alpha(\ell\kappa)^2}{2M_\kappa}+\tfrac{1}{2}\sum_{\alpha\ell\kappa}\sum_{\beta\ell'\kappa'}\phi_{\alpha\beta}(\ell\kappa,\ell'\kappa')u_\alpha(\ell\kappa)u_\beta(\ell'\kappa')\,. \tag{1}$$

When possible we use the notation of Maradudin *et al.*[1] and Eq. (1) is identical with their Eq. (8.3.1). The massless pseudoparticle kinetic energy is set to zero, whereas the potential-energy term is retained,[19] yielding the well-known pseudoparticle zero-mass condition in the equations of motion for fulfillment of the adiabatic approximation.

The Green's-function method[20] is introduced when solving a problem which can be formulated in terms of vibrational correlation functions, e.g., for neutron scattering or impurity vibrations. The basic formalism was described by Zubarev,[21] and was applied to the special case of lattice vibrations by Elliott and Taylor.[5] A review is presented by Elliott *et al.*[22] The Green's-function equation of motion is

$$(\underline{M}\omega^2-\underline{\phi})\underline{G}(\omega)=\underline{I} \tag{2}$$

[cf. Eq. (2.4.42) of Ref. 1]. $\underline{M}$ is the diagonal matrix of particle masses, $\underline{\phi}$ the force-constant matrix, and $\underline{G}(\omega)$ the frequency-dependent Green's-function matrix. In the derivation of Eq. (2) the commutators between the operators $u_\alpha(\ell\kappa)$, $p_\alpha(\ell\kappa)$, and H were used. However, these do not make

sense for massless particles, whose coordinates are entirely determined by the ion coordinates. Therefore, Eq. (2), which is usually taken as the starting point of Green's-function calculations, cannot immediately be applied to phonon models with massless particles. One way to resolve the problem is to realize that the massless particles give just another representation of long-range pure ion-ion interactions. This picture appears impractical, however.

Another formulation assigns a "realistic" mass to the pseudoparticles ($\sim m_e$), and then the usual formalism can be applied to the model. Obviously the adiabatic approximation is violated, but only slightly so, as we can see by a specific example. We introduced a bond charge mass of $2m_e$ into Eq. (2) of Ref. 10 and calculated the phonon dispersion curves for silicon along three symmetry directions in $\vec{k}$ space. The phonon frequencies $\omega_j(\vec{k})$ were changed only $<2\times10^{-5}$ relative to the original calculations. The vibrational modes associated with the bond charges had frequencies between 600 and 2000 THz, compared to the phonon 0–16 THz, indicating that the adiabatic condition is still very well fulfilled. The phonon eigenvectors suffered a relative change $<8\times10^{-5}$ upon introduction of a bond-charge mass. The method described here is not optimal, however, since we are only interested in the ionic vibration frequencies but we nevertheless are forced to solve a significantly larger eigenvalue problem.

Our method takes as the starting point the above description, but explicitly takes the pseudoparticle mass to the limit of zero. Thereby we are still within the adiabatic approximation, even though the formulation is in terms of electronic pseudoparticles representing long-range ionic interactions. We now evaluate the necessary formulas for the Green's functions in this limit. We denote the ions by subscript i and the bond charges by b. The equations of motion (Ref. 10) become

$$M_i\omega^2 u_i = C_{ii}u_i + C_{ib}u_b \ , \tag{3a}$$

$$M_b\omega^2 u_b = C_{ib}^{\dagger}u_i + C_{bb}u_b \ , \tag{3b}$$

which formally apply to a general phonon model employing electronic pseudoparticles. M are the particle masses, C the mass-free dynamical matrix, and u the eigenvectors related to the usual w-type eigenvectors [Eq. (2.1.60) of Ref. 1] by

$$u_i = \vec{w}(i \mid \vec{k}j)/\sqrt{M_i} \ , \tag{4a}$$

$$u_b = \vec{w}(b \mid \vec{k}j)/\sqrt{M_b} \ . \tag{4b}$$

The lattice Green's function solving Eq. (2) is

$$G_{\alpha\beta}(\ell\kappa,\ell'\kappa';\omega) = \frac{1}{N}\sum_{\vec{k}j}\frac{u_\alpha(\kappa \mid \vec{k}j)u_\beta^*(\kappa' \mid \vec{k}j)}{\omega^2-\omega_j^2(\vec{k})} \times e^{i\vec{k}\cdot[\vec{x}(\ell\kappa)-\vec{x}(\ell'\kappa')]} \ , \tag{5}$$

where j is a sum over both ion and bond-charge eigenfrequencies. In the limit $M_b\to0$ we find the following to be true.

(a) $u_i(j=\text{ion})$ is given by the usual formula Eq. (A1) of Ref. 11.

(b) Since both $\vec{w}(i \mid \vec{k},j=\text{ion},b)$ as well as $\vec{w}(i \mid \vec{k},j=\text{ion})$ must satisfy the closure condition [Eq. (2.1.61) of Ref. 1], $\vec{w}(i \mid \vec{k},j=b)$ and $u_i(j=b)$ are zero in this limit.

(c) As usual, $u_b(j=\text{ion}) = -C_{bb}^{-1}C_{ib}^{\dagger}u_i(j=\text{ion})$.

(d) Since $u_i(j=b)$ is zero we find from Eq. (3b)

$$C_{bb}(\vec{k})\cdot\vec{w}(b \mid \vec{k},j=b) = M_b\omega_{j=b}^2(\vec{k})\vec{w}(b \mid \vec{k},j=b) \tag{6}$$

having multiplied by $\sqrt{M_b}$. Thus the eigenvalues of C_{bb} are $\lambda_j = M_b\omega_{j=b}^2$ and the orthonormal eigenvectors are $\vec{w}(b \mid \vec{k},j=b)$.

If we restrict ω to be of the order of a phonon frequency ($\omega << \omega_{j=b}\to\infty$) we obtain for Eq. (5) in the $M_b=0$ limit

$$G_{\alpha\beta}(\ell\kappa,\ell'\kappa';\omega) = \frac{1}{N}\sum_{\vec{k},j=i}\frac{u_\alpha(\kappa \mid \vec{k}j)u_\beta^*(\kappa' \mid \vec{k}j)}{\omega^2-\omega_j^2(\vec{k})}e^{i\vec{k}\cdot[\vec{x}(\ell\kappa)-\vec{x}(\ell'\kappa')]} - \delta_{(\ell\kappa),b}\delta_{(\ell'\kappa'),b}\frac{1}{N}\sum_{\vec{k},j=b}\frac{w_\alpha(\kappa \mid \vec{k}j)w_\beta^*(\kappa' \mid \vec{k}j)}{\lambda_j}e^{i\vec{k}\cdot[\vec{x}(\ell\kappa)-\vec{x}(\ell'\kappa')]} \ . \tag{7}$$

The first term is the usual phonon Green's function, but in addition we find for the bond-charge–bond-charge Green's function an extra term which is seen to originate from the infinite-frequency bond-charge degrees of freedom. This term is a sum involving eigenvalues and eigenvectors of the bond-charge dynamical matrix C_{bb}. Doing the sum over j we find alternatively that the

term can be written as

$$\frac{1}{N}\sum_{\vec{k}}[C_{bb}^{-1}(\vec{k})]_{\alpha\beta}(\ell\kappa,\ell'\kappa')e^{i\vec{k}\cdot[\vec{x}(\ell\kappa)-\vec{x}(\ell'\kappa')]} . \quad (7')$$

This result is in accord with the formulas of Page and co-workers.[14] They used the $M_{\text{shell}}=0$ condition in solving the shell-model Green's function directly from Eq. (2). We have proven that these are *limit* formulas for $M_b\to 0$. We have seen that the extra term actually comes from the infinite electronic frequencies $\omega_{j=b}$ since the product $M_b\omega_{j=b}^2$ nevertheless is finite. Thus it apparently represents a nonadiabatic contribution to the Green's function, corresponding to a term in the phonon density of states at $\omega=\infty$. This is, however, not a discrepancy, since our formulas reflect only a more convenient representation of a long-range-force model *without* pseudoparticles.

B. Substitutional impurity Green's function

The dynamics of a lattice containing a substitutional impurity were described by Elliott and Taylor[5] using Green's functions. Given the perfect-lattice Green's function $\underline{G}(\omega)$ and the mass and force-constant perturbation matrix $\underline{\delta L}(\omega)$ [Eq. (8.3.7) of Ref. 1], the impure-lattice Green's function $\underline{U}(\omega)$ is given by Eq. (8.5.2) of Ref. 1

$$(\underline{I}-\underline{G}\cdot\underline{\delta L})\underline{U}=\underline{G} . \quad (8)$$

Since ω is complex, so are $\underline{G}$, $\underline{\delta L}$, and $\underline{U}$. Usually $\underline{\delta L}$ is assumed to be very localized around the impurity so that the dimension of this equation is quite small. Therefore, the long-range Coulomb forces employed in most semiconductor phonon models present a problem. This was solved by Page and Dick[14] by introducing for each lattice particle a new coordinate representing the electric field. In this way $\underline{\delta L}$ becomes localized around the impurity.

For vibrational correlation functions a dynamic response-function formulation was introduced by Lehman and DeWames,[16] which we shall develop within the current Green's-function framework. Separating the real and imaginary parts of Eq. (8) using Eqs. (A7) and (A9) we arrive at

$$(\underline{I}-\underline{G}\cdot\underline{\delta L})\underline{U} + \left[\frac{\pi}{2\omega}\right]^2(\underline{M}^{-1/2}\underline{g}\underline{M}^{-1/2})\underline{\delta L}(\underline{M}'^{-1/2}\underline{g}'\underline{M}'^{-1/2})=\underline{G} , \quad (9a)$$

$$-(\underline{M}^{-1/2}\underline{g}\underline{M}^{-1/2})\underline{\delta L}\cdot\underline{U} + (\underline{I}-\underline{G}\cdot\underline{\delta L})(\underline{M}'^{-1/2}\underline{g}'\underline{M}'^{-1/2})=(\underline{M}^{-1/2}\underline{g}\underline{M}^{1/2}) \quad (9b)$$

for ω on the real axis. Here, $\underline{g}'(\omega)$ is the generalized density of states for the impure lattice, which is connected to $\underline{U}(\omega)$ via the relations Eqs. (A7) and (A10). The element of $\underline{g}'(\omega)$ referring to the impurity is often called the impurity dynamic response function. $\underline{M}'$ is the diagonal matrix of the impure-lattice masses. From Eq. (9) $\underline{g}'(\omega)$ and $\underline{U}(\omega)$ can be calculated provided we have $\underline{G}(\omega)$ and $\underline{g}(\omega)$ from a phonon model, as well as a model for $\underline{\delta L}(\omega)$. Impurity correlation functions are then calculated from Eq. (B2).

Localized and gap mode contributions can also be treated. In an interval where $\underline{g}(\omega)=0$ we see from Eq. (9b) that $\underline{g}'(\omega)=0$ unless $\det(\underline{I}-\underline{G}\cdot\underline{\delta L})=0$ at some frequency ω_L, in which case $\underline{g}'(\omega)$ may have a delta-function contribution. In Appendix B the calculation of this term is presented.

With Eqs. (9) and (B6) we have specified a method which can be implemented for numerical calculations. A few technical aspects of the numerical calculations are discussed in Appendix C. Symmetry coordinates will also have to be introduced for the matrices involved in order to speed up the computations. For the models with massless particles the mass matrices are usually absorbed into the $\underline{g}(\omega)$ and $\underline{g}'(\omega)$, similar to the formalism in Sec. II A.

C. Impurity Debye temperatures

From the Mössbauer Debye-Waller factor information on the impurity vibrational amplitude can be obtained. Theoretically, we see from Eq. (B2) that $\langle u'_\alpha(00)^2\rangle$ is given in terms of the matrix element $g'_{\alpha\alpha}(00,00;\omega)$ (the impurity dynamic response function), where (00) refers to the impurity site. At high temperatures we get by expanding $\coth(x)$

$$\langle u'_\alpha(00)^2\rangle=\frac{k_BT}{M'_{00}}\left[\mu'(-2)+\frac{1}{12}\left[\frac{\hbar}{k_BT}\right]^2 - \frac{1}{720}\left[\frac{\hbar}{k_BT}\right]^4\mu'(+2)+\cdots\right] . \quad (10)$$

The moments $\mu'(N)$, introduced by Grow *et al.*,[2]

are defined by

$$\mu'(N)=\int_0^\infty \omega^N g'_{\alpha\alpha}(00,00;\omega)d\omega \ . \tag{11}$$

$\mu'(0)=1$ due to Eq. (B3). Defining Debye temperatures[23,2,3] from the $\mu'(N)$

$$\Theta'_D(N)=\frac{\hbar}{k_B}\left[\frac{N+3}{3}\mu'(N)\right]^{1/N}, \quad N\geq -3 \tag{12}$$

we have at high temperatures

$$\langle u'_\alpha(00)^2\rangle=\frac{3k_BT}{M'_{00}}\left[\frac{\hbar}{k_B\Theta'_D(-2)}\right]^2\left[1+\left[\frac{\Theta'_D(-2)}{6T}\right]^2-\left[\frac{\Theta'_D(-2)\Theta'_D(+2)}{60T^2}\right]^2+\cdots\right]. \tag{13}$$

Only the leading term is needed whenever $T>>\frac{1}{6}\Theta'_D(-2)$.

We may derive, as first noted by Lehman and DeWames,[16] $\mu'(-2)$ from Eq. (A7)

$$\mu'(-2)=-M'_{00}U_{\alpha\alpha}(00,00;\omega=0) \ , \tag{14}$$

and similarly for the perfect lattice. Now $\underline{\delta L}(\omega=0)$ equals the force-constant-change matrix $\underline{\Delta\phi}$ [Eq. (8.3.7) of Ref. 1]. Therefore $\underline{U}(\omega=0)$ by Eq. (8) cannot depend on the impurity mass. In terms of Debye temperatures this can be expressed formally as

$$\Theta'_D(-2)=\Theta_D(-2)\left[\frac{M_{00}}{M'_{00}}\right]^{1/2}F(\underline{G};\underline{\Delta\phi}) \ , \tag{15}$$

where $\Theta_D(-2)$ is the host Debye temperature, and F is an unknown function. The impurity $\Theta'_D(-2)$ thus depends on the impurity mass *only* via the square-root term in Eq. (15). Equation (15) implies that different isotopes of the same ion have the same vibrational amplitudes at high temperatures. For the mass-defect model the function becomes $F(\underline{G};\underline{0})=1$, and in the analytical Mannheim model a simple expression for F is found when Eq. (14) is utilized.

The moment $\mu'(+2)$ is given by a simple relation, see, e.g., Eq. (A3) of Ref. 3. In the case of models with massless pseudoparticles it is unfortunately inapplicable, since the high-frequency contributions to $\mu'(+2)$ are not considered in the massless models, cf. Sec. II A. For the perfect lattice, however, it is possible to derive an expression for the high-frequency contributions to the $(+2)$ moment.

III. PARAMETRIZATION OF THE ADIABATIC BOND-CHARGE MODEL

In the following Weber's adiabatic bond-charge model[10,11] (BCM) for silicon, germanium, and α-tin is discussed. The case of diamond is left aside, since the Mössbauer results for this host crystal are still ambiguous.

The BCM parameters were refitted weighting the phonon data according to the experimental errors, contrary to the original fits where special weights were used.[11,13] The four parameters $\frac{1}{3}\phi''_{i-i}$, A_{eff}, β_K, and z^2/ϵ were used for fitting, and we found that the best parameter sets deviated from Weber's[11] sets only by a few percent, except for z^2/ϵ which for α-tin was about 30% larger (Tables I–III). The parameter standard deviations are mostly of the order of one percent, except for α-tin where relatively large experimental error bars are present. The more-accurate silicon and germanium data yield large $\frac{1}{2}\chi^2$ (see Appendix D), thus displaying limitations of the BCM. Some of the maximum possible parameter correlations are uncomfortably close to unity, especially in ger-

TABLE I. Silicon BCM parameters in (e^2/V_a). Fit using 86 phonons (Refs. 34 and 35). Errors in parentheses are standard deviations, and $c_{\max}$ denote the maximum possible correlation coefficient between the parameter and any linear combination of the remaining parameters. $\frac{1}{2}\chi^2$ divided by the number of degrees of freedom indicates the quality of the fit. Further details are given in Appendix D. The CERN computer library program FUMILI (Ref. 33) was used.

	4-parameter model		3-parameter model	
	Value	$c_{\max}$	Value	$c_{\max}$
$\frac{1}{3}\phi''_{i-i}$	6.26(6)	0.48	6.16(4)	0.78
A_{eff}	0.489(4)	0.85	0.487(3)	0.82
β_K	9.17(5)	0.89	9.15(4)	0.89
z^2/ϵ	0.169(3)	0.87	0.173	
$\frac{1}{3}\phi''_{i-\text{BC}}$	6.03		6.16	
$\frac{1}{2}\chi^2/N$	4.11		4.17	

TABLE II. Germanium BCM parameters. Fit using 221 phonons (Refs. 36 and 37). $\vec{k}$ vectors inside the 1 BZ were not included.

	4-parameter model Value	c_{max}	3-parameter model Value	c_{max}
$\frac{1}{3}\phi''_{i-i}$	6.34(2)	0.98	6.495(5)	0.64
A_{eff}	0.340(2)	0.75	0.336(2)	0.67
β_K	9.00(5)	0.93	9.28(3)	0.79
z^2/ϵ	0.215(4)	0.98	0.188	
$\frac{1}{3}\phi''_{i-BC}$	7.40		6.495	
$\frac{1}{2}\chi^2/N$	31.2		31.2	

manium and α-tin. This indicates that the fits are overdetermined. In order to investigate this problem in detail the $\frac{1}{2}\chi^2$ function (Appendix D) was contour plotted in the parameter space for α-tin. Qualitatively the $\frac{1}{2}\chi^2$ function is well behaved, in that it shows elliptical contours, indicating a simple quadratic behavior. The contours also give an indication of the uncertainty in the parameter determination. Strong correlations are present, especially for z^2/ϵ vs $\frac{1}{3}\phi''_{i-i}$ (Fig. 1) and β_K, since narrow valleys cross the parameter planes. However, parameter correlations are in general displayed only indirectly in such contour plots, and a more detailed investigation is warranted in order to understand the correlations underlying Tables I–III. In Appendix D further details are given. We are thus led to conclude that the physical meaning of the parameter trends observed in Ref. 11 is somewhat unclear. Especially z^2/ϵ is strongly coupled to the other parameters, and moreover the values of z are increasing towards α-tin, contrary to intuitive expectation. From this doubt is also cast on the physical contents of parameter trends observed in other semiconductor phonon models, where often as many as 10–15 parameters are involved.

In order to reduce the correlations the BCM parametrization was simplified by proposing *(ad hoc)* that the ion-bond charge parameter $\frac{1}{3}\phi''_{i-BC}$ should equal the ion-ion parameter $\frac{1}{3}\phi''_{i-i}$, since the two parameters describe a similar kind of interaction, and furthermore are seen to be of roughly the same magnitude. Thus the BCM is reduced to a three-parameter model. The new parameter sets are given in Tables I–III, and show only minor changes compared to the four-parameter BCM. It is noteworthy that $\frac{1}{2}\chi^2$ has almost exactly the earlier values. The most important result is that the correlation coefficients are now greatly reduced (see also Appendix D). They are, however, still significant, so that trends in the parameters can only be interpreted with caution. It should be mentioned that these results hardly affect the phonon dispersion curves at all, and that calculations using the four parameters therefore are completely valid.

TABLE III. α-tin BCM parameters. Fit using 62 phonons (Ref. 18).

	4-parameter model Value	c_{max}	3-parameter model Value	c_{max}
$\frac{1}{3}\phi''_{i-i}$	7.3(2)	0.97	7.38(4)	0.58
A_{eff}	0.22(2)	0.78	0.22(1)	0.61
β_K	6.4(3)	0.95	6.5(1)	0.74
z^2/ϵ	0.23(3)	0.98	0.22	
$\frac{1}{3}\phi''_{i-BC}$	7.7		7.38	
$\frac{1}{2}\chi^2/N$	1.13		1.11	

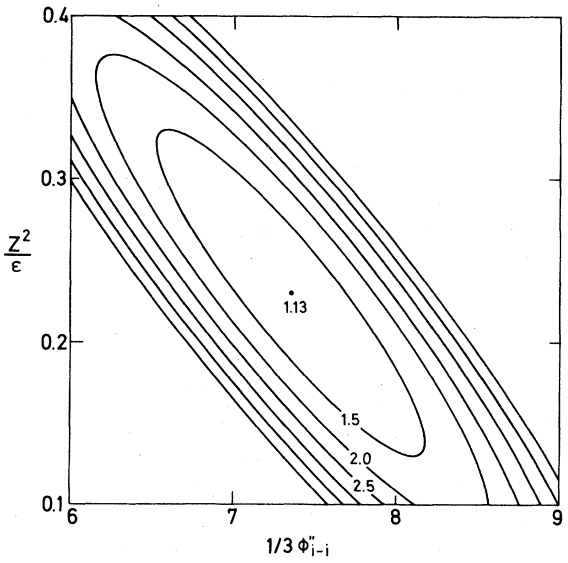

FIG. 1. $\frac{1}{2}\chi^2$ function divided by (62–4) for the 4-parameter α-tin BCM. The inner contour has the value 1.5; the remaining contours represent steps of 0.5. The best-fit point is indicated.

IV. MANNHEIM'S IMPURITY MODEL

The analytical model of Mannheim and co-workers[6] assumes central forces between only nearest neighbors. The model was rederived by Dederichs and Zeller[7] for fcc, bcc, and sc structures, and in Ref. 3 it has been extended to the diamond structure. The derivation in Ref. 3 does not cover zinc-blende structure, as it has been stated, but the important Eq. (26) of Ref. 3 can be shown to hold for this case also. A lattice with nearest-neighbor central forces is unstable, except for fcc.[7] Therefore Mannheim's model should be applied only with caution. For the diamond structure a model was investigated employing central and non-central forces, but even in this case the analytical solution in terms of only the phonon density of states is impossible. This means that for further progress numerically based impurity models are necessary.

V. BOND-CHARGE MODEL OF IMPURITY VIBRATIONS

In a previous paper,[3] current models applicable to the vibrations of substitutional impurities in semiconductors were described. As an extension of this work a model is presented where the impurity vibrates under influence of the same kind of forces as in Weber's adiabatic bond-charge model.[10,11] Specifically, a change in the impurity-host ion-ion coupling $\frac{1}{3}\phi_{i-i}''$, the impurity's bond-bending force β_K and the impurity-bond charge effective coupling A_{eff}, relative to the values of the host lattice is permitted. These are the three parameters which completely characterize the model of the vibrations in the perfect lattice.

The relations between the three parameters and the Born–von Kármán tensor force constants are given by Eqs. (25)–(32) of Ref. 13. The change in long-range Coulomb forces around the impurity is approximated by a short-range potential change within the nearest-neighbor sphere. This seems to be a fairly good approximation in view of the calculation of the germanium phonon dispersion with Coulomb forces beyond nearest neighbors turned off (Fig. 7 of Ref. 11). The general method of Page and co-workers[14] is significantly more complex, and furthermore, the problem of relaxation due to Coulomb force changes is not solved. The short-range Coulomb force-constant changes are easily calculated and added to the change in tensor force constants. The value of z^2/ϵ is given by

$$z^2/\epsilon=\frac{9\sqrt{3}}{512}\left(\tfrac{1}{3}\phi_{i-i}''-A_{\text{eff}}\right). \tag{16}$$

The impurity z'^2/ϵ is also found from Eq. (16) using the impurity parameters. If the host ions have a charge $2z$ and the impurity charge is $2z'$, the bond charge shared between two such ions is $-(z+z')/2$ due to charge neutrality, since the impurity system is assumed to be uncharged. The following changes are obtained in tensor force constants for the impurity, its first-neighbor host ions, and the bond-charge pseudoparticles in between:

$$\Delta\alpha=\Delta\left(\tfrac{1}{3}\phi_{i-i}''\right)+\tfrac{1}{2}\Delta\beta_K\,, \tag{17a}$$

$$\Delta\beta=\Delta\left(\tfrac{1}{3}\phi_{i-i}''\right)-\tfrac{1}{2}\Delta\beta_K - \frac{256}{3\sqrt{3}}\left[\frac{z'(z+z')}{2}-z^2\right]\Big/\epsilon\,, \tag{17b}$$

$$\Delta\mu=\tfrac{1}{4}\Delta\beta_K+2\sqrt{2}\left[\frac{(z+z')^2}{4}-z^2\right]\Big/\epsilon\,, \tag{17c}$$

$$\Delta\nu=\tfrac{1}{4}\Delta\beta_K+6\sqrt{2}\left[\frac{(z+z')^2}{4}-z^2\right]\Big/\epsilon\,, \tag{17d}$$

$$\Delta\delta=\tfrac{1}{4}\Delta\beta_K\,, \tag{17e}$$

$$\Delta\lambda=-\tfrac{1}{4}\Delta\beta_K-4\sqrt{2}\left[\frac{(z+z')^2}{4}-z^2\right]\Big/\epsilon\,, \tag{17f}$$

$$\Delta\alpha'=\Delta\left(\tfrac{1}{3}\phi_{i-i}''\right), \tag{17g}$$

$$\Delta\beta'=\Delta\left(\tfrac{1}{3}\phi_{i-i}''\right)+\frac{64}{3\sqrt{3}}(z'z-z^2)/\epsilon\,, \tag{17h}$$

TABLE IV. Normalized basis vectors for the impurity vibrational mode.

$$\vec{e}_1=\vec{e}_x(000)$$

$$\vec{e}_2=\tfrac{1}{2}[\vec{e}_x(\tfrac{1}{2}\tfrac{1}{2}\tfrac{1}{2})+\vec{e}_x(\tfrac{\bar{1}}{2}\tfrac{\bar{1}}{2}\tfrac{1}{2})+\vec{e}_x(\tfrac{1}{2}\tfrac{\bar{1}}{2}\tfrac{\bar{1}}{2})+\vec{e}_x(\tfrac{\bar{1}}{2}\tfrac{1}{2}\tfrac{\bar{1}}{2})]$$

$$\vec{e}_3=\frac{1}{2\sqrt{2}}[\vec{e}_y(\tfrac{1}{2}\tfrac{1}{2}\tfrac{1}{2})+\vec{e}_z(\tfrac{1}{2}\tfrac{1}{2}\tfrac{1}{2})+\vec{e}_y(\tfrac{\bar{1}}{2}\tfrac{\bar{1}}{2}\tfrac{1}{2})-\vec{e}_z(\tfrac{\bar{1}}{2}\tfrac{\bar{1}}{2}\tfrac{1}{2}) -\vec{e}_y(\tfrac{1}{2}\tfrac{\bar{1}}{2}\tfrac{\bar{1}}{2})-\vec{e}_z(\tfrac{1}{2}\tfrac{\bar{1}}{2}\tfrac{\bar{1}}{2})-\vec{e}_y(\tfrac{\bar{1}}{2}\tfrac{1}{2}\tfrac{\bar{1}}{2})+\vec{e}_z(\tfrac{\bar{1}}{2}\tfrac{1}{2}\tfrac{\bar{1}}{2})]$$

$$\vec{e}_4=\tfrac{1}{2}[\vec{e}_x(111)+\vec{e}_x(\bar{1}\bar{1}1)+\vec{e}_x(1\bar{1}\bar{1})+\vec{e}_x(\bar{1}1\bar{1})]$$

$$\vec{e}_5=\frac{1}{2\sqrt{2}}[\vec{e}_y(111)+\vec{e}_z(111)+\vec{e}_y(\bar{1}\bar{1}1)-\vec{e}_z(\bar{1}\bar{1}1) -\vec{e}_y(1\bar{1}\bar{1})-\vec{e}_z(1\bar{1}\bar{1})-\vec{e}_y(\bar{1}1\bar{1})+\vec{e}_z(\bar{1}1\bar{1})]$$

TABLE V. Perfect lattice Green's function in the impurity vibration subspace. The matrix is symmetric.

G_1				
$2G_2$	$(G_4+G_6+2G_8)$			
$2\sqrt{2}G_3$	$\sqrt{2}(G_5+G_9)$	$(G_4+G_5-G_6-2G_7-G_9)$		
$2G_{10}$	$(G_2+G_{12}+2G_{14})$	$\sqrt{2}(G_3-G_{13}+G_{15}-G_{16})$	$(G_1+2G_{17}+G_{20})$	
$2\sqrt{2}G_{11}$	$\sqrt{2}(G_3+G_{13}+G_{15}+G_{16})$	$(G_2+G_3-G_{12}+G_{13}-G_{15}-G_{16})$	$\sqrt{2}G_{19}$	$(G_1+2G_{18}-G_{19}-G_{20})$

Here, e.g., $\Delta\alpha=\alpha_{\text{imp}}-\alpha_{\text{host}}$. The first derivatives of the potentials ϕ_{i-i} and $\phi_{i-\text{BC}}$ [cf. Eqs. (23) and (24) of Ref. 13] are unchanged in the present approximation. If the true long-range Coulomb forces were changed, the first derivative of the Coulomb energy would cause a relaxation around the impurity.

The force-constant changes are limited to within the first neighbors of the impurity, and the dimension of Eq. (8) becomes 27. This is reduced to 5 if the symmetry coordinates given in Table IV are used. These are analogous to the F_2-mode coordinates of the zinc-blende structure given by Ludwig.[24] In this subspace both the perfect-lattice Green's functions $\underline{G}(\omega)$ and $\underline{g}(\omega)$ and the first column of the impurity Green's functions $\underline{U}(\omega)$ and $\underline{g}'(\omega)$ are given as in Table V. The matrix $\underline{\delta L}(\omega)$ is similar, but contains a few modifications (Table VI). The labeling of the matrix elements is defined in Table VII.

The numerical calculations are performed as follows. The impurity force constants are set equal to three different scale factors times the host lattice $\frac{1}{3}\phi'_{-i}$, β_K, and A_{eff}. From Eq. (12), Ref. 13, and Eq. (8.3.7) of Ref. 1, $\underline{\delta L}(\omega)$ can be constructed. The impurity mass is also known. $\underline{G}(\omega)$ and $\underline{g}(\omega)$ are calculated as described in Appendix C. In the present calculations 609 $\vec{k}$ vectors were used, corresponding to 20 480 microtetrahedra, in the irreducible first Brillouin zone (1 BZ). From Eqs. (9) and (B6) the impurity density of states $\underline{g}'(\omega)$ is calculated, and the impurity dynamic response function $g'_{\alpha\alpha}(000,000;\omega)$ is found. This procedure may be performed for any combination of the three force-constant scale factors. In particular, the mass-defect result can be calculated and compared with the analytical result [Eq. (20) of Ref. 3]. The Kramers-Krönig relations [Eqs. (A7) and (A10)] may be used to check the Green's functions and density of states functions.

VI. RESULTS AND DISCUSSION

Calculations were performed for the isoelectronic ^{119}Sn impurity in silicon and germanium. ^{119}Sn in α-tin was treated adequately in Ref. 3, since ^{119}Sn is not an impurity in this case. For completeness, however, results for an isovalent impurity in α-tin are also presented. The remaining two cases are relatively heavy impurities whose dynamic response functions will have dominant contributions at low frequencies (a resonance mode) compared to host lattice frequencies (Fig. 2). Localized modes will not be present for realistic force-constant changes. The "analytic" behavior of the model is investigated by discussing the consequences of decreasing individually the three impurity force constants towards zero. The force-constant changes were approximated, as described above, to extend to first-nearest neighbors only.

A change in the impurity-bond charge coupling A_{eff} had only a small effect, in contrast to the perfect lattice where the phonon frequency $\omega^2_{\text{TA}}(X)$ is roughly proportional[11] to A_{eff}. For the impurity, however, setting $A_{\text{eff}}=0$ only decreased the Debye temperature $\Theta'_D(-2)$ by about 5% (Fig. 3). The reason is that the bond-bending forces and the host-lattice Coulomb forces are still sufficient to

TABLE VI. Force-constant-change matrix $\underline{\delta L}$ in the impurity vibration subspace. Equation (8.3.9) of Ref. 1 was utilized. $\underline{\delta L}$ is symmetric.

δL_1				
$2\delta L_2$	$-\delta L_2$			
$2\sqrt{2}\delta L_3$	$-\sqrt{2}\delta L_3$	$-[\delta L_2+\delta L_3+2(\delta L_6+\delta L_7+\delta L_8+\delta L_9)]$		
$2\delta L_{10}$	0	0	$-\delta L_{10}$	
$2\sqrt{2}\delta L_{11}$	0	0	$-\sqrt{2}\delta L_{11}$	$-(\delta L_{10}+\delta L_{11})$

TABLE VII. Definition of matrix elements in Tables V and VI.

$G_1=G_{xx}(000,000;\omega)$	$G_{11}=G_{xy}(111,000;\omega)$
$G_2=G_{xx}(\frac{1}{2}\frac{1}{2}\frac{1}{2},000;\omega)$	$G_{12}=G_{xx}(111,\frac{1}{2}\frac{\bar{1}}{2}\frac{\bar{1}}{2};\omega)$
$G_3=G_{xy}(\frac{1}{2}\frac{1}{2}\frac{1}{2},000;\omega)$	$G_{13}=G_{xy}(111,\frac{1}{2}\frac{\bar{1}}{2}\frac{\bar{1}}{2};\omega)$
$G_4=G_{xx}(\frac{1}{2}\frac{1}{2}\frac{1}{2},\frac{1}{2}\frac{1}{2}\frac{1}{2};\omega)$	$G_{14}=G_{yy}(111,\frac{1}{2}\frac{\bar{1}}{2}\frac{\bar{1}}{2};\omega)$
$G_5=G_{xy}(\frac{1}{2}\frac{1}{2}\frac{1}{2},\frac{1}{2}\frac{1}{2}\frac{1}{2};\omega)$	$G_{15}=G_{yz}(111,\frac{1}{2}\frac{\bar{1}}{2}\frac{\bar{1}}{2};\omega)$
$G_6=G_{xx}(\frac{1}{2}\frac{1}{2}\frac{1}{2},\frac{1}{2}\frac{\bar{1}}{2}\frac{\bar{1}}{2};\omega)$	$G_{16}=G_{yx}(111,\frac{1}{2}\frac{\bar{1}}{2}\frac{\bar{1}}{2};\omega)$
$G_7=G_{yx}(\frac{1}{2}\frac{1}{2}\frac{1}{2},\frac{1}{2}\frac{\bar{1}}{2}\frac{\bar{1}}{2};\omega)$	$G_{17}=G_{xx}(111,\bar{1}1\bar{1};\omega)$
$G_8=G_{yy}(\frac{1}{2}\frac{1}{2}\frac{1}{2},\frac{1}{2}\frac{\bar{1}}{2}\frac{\bar{1}}{2};\omega)$	$G_{18}=G_{yx}(111,\bar{1}1\bar{1};\omega)$
$G_9=G_{yz}(\frac{1}{2}\frac{1}{2}\frac{1}{2},\frac{1}{2}\frac{\bar{1}}{2}\frac{\bar{1}}{2};\omega)$	$G_{19}=G_{xz}(111,\bar{1}1\bar{1};\omega)$
$G_{10}=G_{xx}(111,000;\omega)$	$G_{20}=G_{yy}(111,\bar{1}1\bar{1};\omega)$

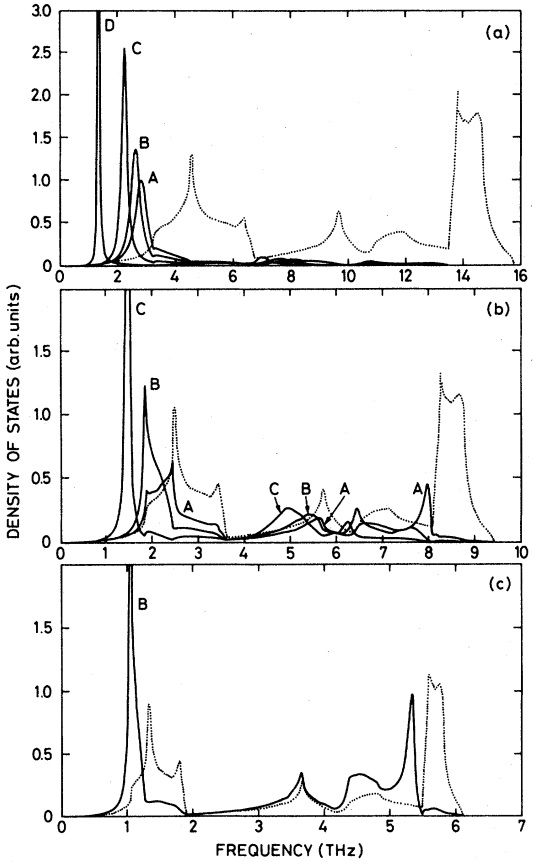

FIG. 2. Impurity dynamic response function for ^{119}Sn in (a) silicon, (b) germanium, and (c) α-tin. Force-constant ratios are 1.0 (A, mass-defect case), 0.8 (B), 0.6 (C), and 0.4 (D). Dotted curves are the phonon density of states.

stabilize the impurity and its bond charges. Also, Eq. (8) shows that the matrix $\underline{\delta L}$ determines the impurity vibrations, and since A_{eff} numerically is very small, the force-constant part of $\underline{\delta L}$ differs only very little from the zero matrix.

Changing the bond-bending potential β_K of the impurity also resulted in moderate deviations in impurity Debye temperature. Setting the impurity $\beta_K=0$ decreased the $\Theta'_D(-2)$ by about 10%. For the perfect lattice case, a BCM for silicon was calculated setting $\beta_K=0$, and the TA and LA frequencies were lowered by 50% and 20%, respectively. The optical phonons showed minor changes. The Coulomb potentials in both cases stabilize the bond angles sufficiently to prevent a structural transition of the impurity or the crystal.[25]

The impurity-host ion-ion central potential $\frac{1}{3}\phi''_{-i}(=\frac{1}{3}\phi''_{-\text{BC}})$ significantly affected the impurity vibrations when being changed. At an impurity-to-host force-constant ratio between 0 and 0.6, its frequency becomes imaginary. For the perfect lattice a change in $\frac{1}{3}\phi''_{-i}$ mainly modifies the optical phonons, and only at $\frac{1}{3}\phi''_{-i}=0$ does the lattice become unstable.

Simultaneous decrease of all impurity forces diminishes the $\Theta'_D(-2)$ slightly faster than with a decrease of $\frac{1}{3}\phi''_{-i}$, indicating that the ion-ion and ion—bond-charge central force is the most important parameter governing the impurity vibrations. The impurity becomes unstable when the force constant ratio is lowered to between 0.3 and 0.6,

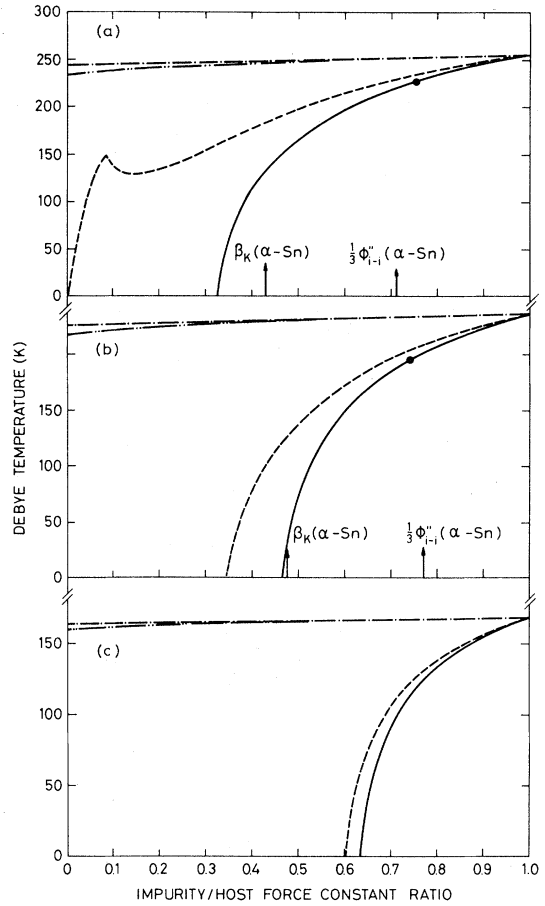

FIG. 3. Debye temperatures for ^{119}Sn in (a) silicon, (b) germanium, and (c) α-tin for force-constant ratios from 0−1. The changes are in all potentials (——), $\frac{1}{3}\phi''_{i-i}$ (— — —), β_K (—··—), and A_{eff}(—·—·—·). The Mössbauer data are shown (●), as are β_K and $\frac{1}{3}\phi''_{i-i}$ for the α-tin lattice, converted into host-lattice units.

the instability first being reached in α-tin.

The moderate decreases in $\Theta'_D(-2)$ when A_{eff} and β_K are changed are not surprising, as argued above, but so is the impurity's instability at first sight when $\frac{1}{3}\phi''_{i-i}$ is decreased to some finite value. This may result from the short-range approximation of the change in Coulomb forces, which had to be assumed for computational simplicity. This is illustrated by the following example: A BCM for germanium with Coulomb forces beyond the nearest-neighbor atoms turned off was calculated, yielding phonon dispersion quite similar to the full BCM.[11] Impurity calculations within this model along the lines of Sec. V do not contain any approximations, and it was indeed found that only when all impurity forces were decreased to zero did the impurity become unstable. This is the intuitively expected model behavior, representing a vacancy defect. On the other hand, it is well known that the effective forces for TA modes represent close cancellations of strong covalent and Coulomb forces, and changing impurity charges may thus very well introduce instabilities that would not occur in the simplified models with short-range forces only.

A physical description of the situation close to impurity instability can be indicated by the scattering of lattice phonons off the impurity [Eq. (8.3.72) of Ref. 1]. It is easy to show that the scattered wave $\vec{w}$ is given by

$$\vec{w}=\underline{U}\cdot\underline{\delta L}\cdot\vec{u}_0\,, \tag{18}$$

where $\vec{u}_0$ is the incoming phonon wave. Considering long-wavelength acoustical phonons ($\omega\approx 0$), it can be shown within our model that $\underline{\delta L}\cdot\vec{u}_0$ is close to zero, but finite for $k\neq 0$ (Γ). From Eq. (9) it is seen that both the real and imaginary parts of $\underline{U}$ become almost infinite if $\det(\underline{I}-\underline{G}\cdot\underline{\delta L})=0$ for $\omega\approx 0$, and as a result arbitrarily large scattered waves are generated. This means that the long-wavelength acoustical phonons are scattered with almost infinite strength by the impurity, thus leading to its instability if a resonance mode occurs at $\omega\approx 0$.

Turning to the interpretation of Mössbauer experiments, $\Theta'_D(-2)$ for ^{119}Sn was calculated as function of the impurity-to-host force-constant ratio. In Fig. 3 $\Theta'_D(-2)$ is shown versus the ratios of the impurity force constants to the host-lattice values. Simultaneous scaling of all three parameters is also shown. It should be noted that the force-constant changes for other isovalent impurities than ^{119}Sn can be found by scaling the ordinates of Fig. 3 by an appropriate mass ratio [cf. Eq. (15)].

The experimental values of $\Theta'_D(-2)$ for ^{119}Sn in silicon and germanium taken from Ref. 3 are indicated, yielding the actual force-constant weakening at the impurity (Table VIII). It is interesting to compare the impurity's force constants with the values from the α-tin perfect lattice (Table III), converted to the host-lattice units (Table VIII). Linear interpolation of impurity forces from the host values down to the α-tin values showed that the impurity $\Theta'_D(-2)$ are reproduced by some intermediate force-constant values. These are quite near to the α-tin values, as might be expected from Fig. 3. It therefore appears that the ^{119}Sn impurity

TABLE VIII. Force constants of ^{119}Sn and α-tin relative to silicon and germanium.

Host	$\frac{\phi(^{119}\text{Sn-host})}{\phi(\text{host})}$	$\frac{1}{3}\phi''_{i-i}$	$\frac{\phi(\alpha-\text{tin})}{\phi(\text{host})}$ A_{eff}	β_K
Silicon	0.74(2)	0.71	0.27	0.42
Germanium	0.73(2)	0.76	0.44	0.47

to some extent retains its α-tin character when it is embedded substitutionally in silicon and germanium. This interpretation does not accord with the picture[26,27] that the Sn impurity has an electronic structure which resembles that of the host material. On the other hand, vibrational and electronic properties are not immediately connected, and the difference is not a contradiction.

When scaling down all impurity parameters by the same factor, which we believe is the most realistic procedure for interpretation of experiments, the impurity $\Theta'_D(-2)$ decreases. Force-constant weakenings of about 25% are concluded in both silicon and germanium (Table VIII). The moderate force-constant weakenings accord with an intuitive picture, where the α-tin force constants should represent lower bounds, and some intermediate values should be more probable.

In contrast, Mannheim's model for the same systems showed force constant weakening far below the α-tin values (Table VI of Ref. 3). It is thus found that the Mannheim model force-constant ratios do not carry the physical significance that the model assigns to them.

Experimental results for localized mode frequencies (cf. Sec. II B) are available for the isovalent impurities C in Si and Si in Ge. Using the adiabatic bond-charge model together with the simple mass-defect model[3] yields the frequencies 616 cm^{-1} (^{12}C), 598 cm^{-1} (^{13}C), and 582 cm^{-1} (^{14}C) in Si, and 382 cm^{-1} (^{28}Si) in Ge. The experimentally determined frequencies[38] differ slightly from these predictions. With the present impurity model, using Eq. (B4), the experimental values were fitted when scaling all the impurity potentials by the factors 0.96 (C in Si) and 1.04 (Si in Ge). These force-constant changes are much smaller than those for Sn in Si and Ge, suggesting differences in the impurity-host interactions of a Sn impurity compared with C or Si impurities.

VII. CONCLUSION

It was shown that Green's functions for phonon models with massless pseudoparticles can be calculated by the usual methods, taking into account an extra constant term in the Green's function. The correct Kramers-Krönig relations for phonon Green's functions are shown in Appendix A. Expressions convenient for actual calculations of Green's functions were presented.

The number of parameters in Weber's adiabatic bond-charge model was reduced to 3. Difficulties were experienced in assigning direct physical meaning to the phonon model parameters. The parameters of the BCM do not show unambiguous trends, especially because significant parameter correlations are found using the available phonon dispersion data for silicon, germanium, and α-tin. Considering also that the fits obtained are not "perfect," perhaps different or extra interactions should be introduced in order to improve the BCM description of the group-IV semiconductors. Anharmonic contributions to the experimental phonon frequencies could also play a role.

A model was presented changing the BCM forces around a substitutional impurity. The changes were approximated to extend to first-nearest neighbors only, neglecting the change in long-range Coulomb forces. Comparison with experimental impurity Debye temperatures $\Theta'_D(-2)$ showed, by the mass-defect model,[3] the existence, within the harmonic approximation, of force-constant weakening around a ^{119}Sn substitutional impurity in silicon and germanium. Within our impurity bond-charge model the experimental $\Theta'_D(-2)$ are fitted if the impurity potentials are scaled by the factors 0.74(2) in silicon and 0.73(2) in germanium. These values lie between the host and the α-tin force constants, being closer to the α-tin values. Localized mode frequencies for isovalent C in Si and Si in Ge showed only 4% force-constant changes, suggesting differences in the impurity-host interactions compared to the Sn impurity.

The force-constant change was also quantified in Ref. 3 by means of Mannheim's model, whereby a decrease of about a factor 0.5 compared to the host-lattice force constants was concluded. However, in our opinion a rigorous interpretation of results obtained from Mannheim's model for semiconductors gives qualitatively as well as quantitatively misleading conclusions.

We believe that the isoelectronic ^{119}Sn substitutional impurity in silicon, germanium, and α-tin is now quite well understood from the complementary electronic structure and lattice-dynamical viewpoints. The systems treated here must be considered the simplest possible impurity-semiconductor combinations. Whether nonisovalent impurities in the same hosts or impurities in the polar semiconductors can also yield simple pictures is still an open question.

ACKNOWLEDGMENTS

The guidance of E. Antoncik and W. Weber in this work is gratefully acknowledged. Discussions on several technical points with D. Strauch, A. Holst Andersen, and H. C. Fogedby were most fruitful. The collaboration with J. W. Petersen, S. Damgaard, and G. Weyer on the interpretation of Mössbauer data was a constant stimulus.

APPENDIX A: KRAMERS-KRÖNIG RELATIONS

The relations between the real and imaginary parts of a Green's function are in part of the literature inconsistent. This work refers to the basic work of Zubarev.[21]

An arbitrary Green's function $G(z)$ is analytic in the complex frequency plane ($z=\omega+i\gamma$) except for a branch cut on the real axis. For physical systems without damping the branch cut consists of a set of discrete poles in $G(z)$ at the normal-mode frequencies of the system. In the upper z half-plane $G(z)$ is called the *retarded* Green's function $G_R(z)$, and in the lower z half-plane it is called the *advanced* Green's function $G_A(z)$. The real and imaginary parts of $G_A(\omega)$ are connected by Eq. (3.31) of Ref. 21:

$$\mathrm{Re}G_A(\omega)=\frac{1}{\pi}\mathscr{P}\int_{-\infty}^{\infty}d\omega'\frac{\mathrm{Im}G_A(\omega')}{\omega-\omega'}\ , \tag{A1}$$

$$\mathrm{Im}G_A(\omega)=-\frac{1}{\pi}\mathscr{P}\int_{-\infty}^{\infty}d\omega'\frac{\mathrm{Re}G_A(\omega')}{\omega-\omega'} \tag{A2}$$

in the limit where ω and ω' approach the real axis from below. $\mathscr{P}\int$ denotes a Cauchy principal-value integral. For finite systems $\mathrm{Im}G_A(\omega')$ is a sum of δ functions, which have to be smoothed over sufficiently small intervals $\Delta\omega$ in order for Eqs. (A1) and (A2) to have any meaning.[28] The corresponding relations for $G_R(\omega)$ have just the opposite signs.

For phonon systems one can prove the symmetry properties[28]

$$\mathrm{Re}G_A(\omega)=\mathrm{Re}G_A(-\omega)\ , \tag{A3}$$

$$\mathrm{Im}G_A(\omega)=-\mathrm{Im}G_A(-\omega)\ . \tag{A4}$$

From these relations we may write

$$\mathrm{Re}G_A(\omega)=\frac{1}{\pi}\mathscr{P}\int_0^{\infty}d\omega'\frac{2\omega'\,\mathrm{Im}G_A(\omega')}{\omega^2-\omega'^2}\ , \tag{A5}$$

$$\mathrm{Im}G_A(\omega)=-\frac{2\omega}{\pi}\mathscr{P}\int_0^{\infty}d\omega'\frac{\mathrm{Re}G_A(\omega')}{\omega^2-\omega'^2}\ . \tag{A6}$$

In the phonon literature the real part of the advanced Green's functions is usually defined as

$$\underline{G}(\omega)=G_{\alpha\beta}(\ell\kappa,\ell'\kappa';\omega)=\frac{1}{\sqrt{M_{\ell\kappa}M_{\ell'\kappa'}}}\mathscr{P}\int_0^{\infty}d\omega'\frac{g_{\alpha\beta}(\ell\kappa,\ell'\kappa';\omega')}{\omega^2-\omega'^2}\ , \tag{A7}$$

where $g_{\alpha\beta}(\ell\kappa,\ell'\kappa';\omega)$ is a smooth *generalized density-of-states* function [cf. Eqs. (2.4.44) and (8.5.5) of Ref. 1]. For example, for the perfect lattice we have

$$\underline{g}(\omega)=g_{\alpha\beta}(\ell\kappa,\ell'\kappa';\omega)=\frac{1}{N}\sum_{\vec{k}j}w_\alpha(\kappa\mid\vec{k}j)w_\beta(\kappa'\mid\vec{k}j)^*e^{i\vec{k}\cdot[\vec{x}(\ell\kappa)-\vec{x}(\ell'\kappa')]}\delta(\omega-\omega_j(\vec{k}))\ . \tag{A8}$$

From Eqs. (A5), (A6), and (A7) we obtain the result

$$\frac{g_{\alpha\beta}(\ell\kappa,\ell'\kappa';\omega)}{\sqrt{M_{\ell\kappa}M_{\ell'\kappa'}}}=\frac{2\omega}{\pi}\mathrm{Im}G_{\alpha\beta}(\ell\kappa,\ell'\kappa';\omega) \tag{A9}$$

$$=-\left[\frac{2\omega}{\pi}\right]^2\mathscr{P}\int_0^{\infty}d\omega'\frac{G_{\alpha\beta}(\ell\kappa,\ell'\kappa';\omega')}{\omega^2-\omega'^2}\ , \tag{A10}$$

where the advanced Green's function is understood. The equations (A7) and (A10) we shall call the

Kramers-Krönig relations, since they couple $\underline{G}(\omega)$ and $\underline{g}(\omega)$. They apply to any collection of harmonically coupled particles. We note that, for instance, the relations (2.24)–(2.26) of Ref. 7 are inconsistent.[29]

APPENDIX B: CORRELATION FUNCTIONS AND LOCALIZED MODES

We start from the fluctuation-dissipation theorem [Eq. (3.28) of Ref. 21] for the thermal average of two operators $A(t)$ and $B(t'=0)$:

$$\langle A(t)B(0)\rangle = \lim_{\epsilon\to 0+} \frac{i\hbar}{2\pi}\int_{-\infty}^{\infty} d\omega \frac{e^{\hbar\omega/k_BT}}{e^{\hbar\omega/k_BT}-1} e^{-i\omega t}[G(\omega+i\epsilon)-G(\omega-i\epsilon)] , \tag{B1}$$

where $G(z)$ is the Green's function of the operators and T is the ensemble temperature. The factor 2π is in accord with the standard phonon formulas of, e.g., Elliott *et al.*[22] The square bracket equals $-2i[\mathrm{Im}G_A(\omega)]$, so the integral is only over the finite interval between $+$ and $-$ the maximum lattice frequency. Using Eq. (A9) we may write, e.g., the equal-time displacement correlation functions

$$\langle u_\alpha(\ell\kappa)u_\beta(\ell'\kappa')\rangle = \frac{\hbar}{2\sqrt{M_{\ell\kappa}M_{\ell'\kappa'}}}\int_0^\infty \frac{1}{\omega} g_{\alpha\beta}(\ell\kappa,\ell'\kappa';\omega)\coth(\tfrac{1}{2}\hbar\omega/k_BT)d\omega \tag{B2}$$

which corresponds to Eq. (8.6.4a) of Ref. 1. From Eq. (8.6.4c) of Ref. 1 $\underline{g}(\omega)$ satisfies the normalization condition

$$\int_0^\infty d\omega\, g_{\alpha\beta}(\ell\kappa,\ell'\kappa';\omega)=\delta_{\alpha\beta}\delta_{\ell\ell'}\delta_{\kappa\kappa'} . \tag{B3}$$

The particles are assumed to have nonzero masses, and the result applies to any harmonic system, including the substitutional impurity system.

The properties of an impurity localized vibrational mode at the frequency ω_L is found via Eq. (4):

$$\underline{g}(\omega)=0, \quad (\underline{I}-\underline{G}\cdot\underline{\delta}\,\underline{L})\underline{U}=\underline{G} ,$$

$$\det(\underline{I}-\underline{G}\cdot\underline{\delta}\,\underline{L})=0 . \tag{B4}$$

The standard solution of linear equations may then be expressed as

$$\underline{U}=\underline{\Delta}/\det(\underline{I}-\underline{G}\cdot\underline{\delta}\,\underline{L}) \tag{B5}$$

with the well-known algorithm for calculating $\underline{\Delta}$. The delta-function contribution to $\mathrm{Im}U_A(\omega)$ from the localized mode is calculated as follows: Sufficiently close to $+$ or $-\omega_L$, $U_A(z)=C(z^2-\omega_L^2)^{-1}$, C being a constant. $U_A(z)$ thus has a pole of order $1/z$ at ω_L, giving

$$\mathrm{Im}\lim_{z\to\omega_L} U_A(z)=C\pi/2\omega_L\delta(z-\omega_L) .$$

Assuming the zero of $\det(\underline{I}-\underline{G}\cdot\underline{\delta}\,\underline{L})$ to be of first order we obtain the localized mode contribution to the impurity density of states

$$\underline{g}'(\omega)=2\omega\underline{M}'^{1/2}\underline{\Delta}\,\underline{M}'^{1/2}\left[\frac{d}{d\omega}\det(\underline{I}-\underline{G}\cdot\underline{\delta}\,\underline{L})\right]^{-1}$$

$$\times\delta(\omega-\omega_L) . \tag{B6}$$

APPENDIX C: NUMERICAL METHODS FOR GREEN'S FUNCTIONS

The generalized density of states Eq. (A8) is calculated numerically by integration over the Brillouin zone. Such methods were reviewed by Gilat,[30] but the inclusion of weight factors in front of the delta function have not received much attention in the literature. Recently MacDonald *et al.*[31] presented a hybrid tetrahedron scheme which interpolates linearly both eigenfrequencies and weight factors within the microtetrahedra. Quadratic interpolation enables a subdivision of the microtetrahedra. The interpolant function is continuous between adjacent tetrahedra. This is not a property of many of the available schemes. We found by numerical tests that their expressions for densities of states lead to inaccurate results when only few or no constant-frequency planes intersect the given microtetrahedron. However, their formulas for the number of states gave very accurate results when the contributions were divided into separate bins so as to yield the density of states. The "+" in their Eq. (2.7d) is a misprint and should be a "−." This method seems to us to be one of the most ac-

curate and generally applicable schemes available at present for Brillouin-zone sums.

The sum in Eq. (A8) must be reduced to a sum over the irreducible part of the Brillouin zone by means of symmetry, e.g., by Eq. (3.3.6b) of Ref. 1. This equation can be reformulated for the w-type eigenvectors [Eq. (2.1.59) of Ref. 1] as

$$w_\alpha(\kappa \mid \underline{S}\vec{k}j)=\sum_\beta S_{\alpha\beta} w_\beta(F_0(\kappa,S^{-1}) \mid \vec{k}j) \ . \quad \text{(C1)}$$

A trivial phase factor may multiply the right-hand side. The function F_0 is defined by Eq. (3.2.12) of Ref. 1. Eigenvectors at $-\vec{k}$ are given by Eq. (2.1.57) of Ref. 1, and if we consider only operations which do not contain the inversion we obtain

$$g_{\alpha\beta}(\ell\kappa,\ell'\kappa';\omega)=\frac{1}{N}\sum_{\vec{k}j}{}'\sum_S\sum_{\mu\nu} S_{\alpha\mu}S_{\beta\nu}\,2\,\mathrm{Re}[w_\mu(F_0(\kappa,S^{-1}) \mid \vec{k}j)w_\nu(F_0(\kappa',S^{-1}) \mid \vec{k}j)^* \times\exp\{i\underline{S}\vec{k}\cdot[\vec{x}(\ell\kappa)-\vec{x}(\ell'\kappa')]\}]\delta(\omega-\omega_j(\vec{k})) \ . \quad \text{(C2)}$$

The sum $\sum'$ is over the irreducible part of the Brillouin zone.

Principal value integrals, Eqs. (A7) and (A10) present a numerical problem. Instead of the sometimes applied method of going a finite step into the complex frequency plane, we have developed a procedure exact up to second order in the integrand.

It is readily proven that in an interval $[a;b]$ where $f(x')$ is approximated by an (at most) quadratic interpolant $\bar{f}(x')=\alpha+\beta x'+\gamma x'^2$ we have

$$\mathcal{P}\int_a^b \frac{1}{x^2-x'^2}f(x')dx'=\frac{1}{2x}\bar{f}(x)\ln\left|\frac{x+b}{x-b}\frac{x-a}{x+a}\right|+\beta\ln\left|\frac{x+a}{x+b}\right|+\gamma(a-b) \quad \text{(C3)}$$

for any $x\neq +$ or $-a$, $+$ or $-b$. When the interpolant $\bar{f}(x')$ is continuous in two subsequent intervals, it may be seen that (C3) is also valid at their common endpoint, since the divergent terms cancel. The numerical accuracy can be checked by the Kramers-Krönig relations. The high-frequency expansion of $\underline{G}(\omega)$, Eq. (2.61) of Ref. 7, may be useful for doing the infinite integral Eq. (A10).

Numerical diagonalization of Hermitian matrices has by now been well investigated.[32] However, old algorithms that are both slow and inaccurate are still widely applied. For example, we

TABLE IX. Elements of the covariance matrix corresponding to the fits in Tables I–III. We have numbered the parameters $1=\frac{1}{3}\phi'_{i-i}$, $2=A_{\text{eff}}$, $3=\beta_K$, $4=z^2/\epsilon$.

	Silicon		Germanium		α-tin	
Number of Data	86	86	221	221	62	62
Number of parameters	4	3	4	3	4	3
σ_1	0.0557	0.0449	0.0197	0.0047	0.1880	0.0439
σ_2	0.0036	0.0034	0.0018	0.0016	0.0144	0.0116
σ_3	0.0452	0.0428	0.0450	0.0283	0.2974	0.1360
σ_4	0.0027		0.0034		0.0312	
c_{12}	0.1687	−0.0058	−0.3319	0.2824	−0.5154	0.2220
c_{13}	−0.2604	−0.5831	0.6803	−0.6198	0.8086	−0.5477
c_{14}	−0.0867		−0.9611		−0.9621	
c_{23}	−0.5043	−0.6622	−0.6943	−0.6556	0.7358	−0.6014
c_{24}	−0.2981		0.4059		0.5722	
c_{34}	−0.5298		−0.8024		0.8979	

found that certain Jacobi methods were unreliable, and in the present work we used a version of the considerably better Householder's method. Available subroutine packages are discussed by Parlett.[32]

APPENDIX D: DETERMINATION OF PARAMETERS

Parameter determination for a model is often performed by minimizing the $\frac{1}{2}\chi^2$ function (least-squares sum)

$$\frac{1}{2}\chi^2=\sum_i (y_{i,\text{model}}-y_{i,\text{expt}})^2/2\Delta y_i^2 , \tag{D1}$$

where Δy_i is the experimental error, using a given set of data. A large variety of computer programs exist for this purpose, generally being based on similar ideas. The better programs (e.g., FUMILI which is available from CERN[33]) provide also the so-called covariance-matrix of the fit.

For an optimum parameter set $\hat{\theta}=(\hat{\theta}_1,\ldots,\hat{\theta}_N)$ the covariance matrix $\text{cov}(\hat{\theta})$ has the symmetric elements $(c_{ij}\sigma_i\sigma_j)$. σ_i is the ith parameter standard deviation, and c_{ij} is the correlation coefficient between the parameters $\hat{\theta}_i$ and $\hat{\theta}_j$ ($c_{ii}=1$). The matrix $\text{cov}(\hat{\theta})$ is related to the $\frac{1}{2}\chi^2$ function as follows: The quadratic expansion of $\frac{1}{2}\chi^2(\theta)$ around $\hat{\theta}$ is given by

$$\frac{1}{2}\chi^2(\theta)=\frac{1}{2}\chi^2(\hat{\theta}) + \frac{1}{2}\sum_{i,j=1}^{N}(\theta_i-\hat{\theta}_i)[\text{cov}(\hat{\theta})^{-1}]_{ij}(\theta_j-\hat{\theta}_j) , \tag{D2}$$

where θ are the parameter variables. This expansion may or may not be a good approximation to the actual $\frac{1}{2}\chi^2$ function, a point which always must be investigated. It is seen from Eq. (D2) that the correlation coefficients c_{ij} only influence the $\frac{1}{2}\chi^2$ function through the inverse of $\text{cov}(\hat{\theta})$, and hence contour plots in general yield only very indirect information on parameter correlations.

For the BCM parameter fits of Sec. III we found the quadratic expansion to be very good (to within a few percent), when going as far as 25% away from the optimum points. Hence Tables I–III together with $\text{cov}(\hat{\theta})$ contain all the information necessary to make a complete series of contour plots of $\frac{1}{2}\chi^2(\theta)$. In Table IX we give the standard deviations and correlation coefficients entering $\text{cov}(\hat{\theta})$.

[1] A. A. Maradudin, E. W. Montroll, G. H. Weiss, and I. P. Ipatova, *Theory of Lattice Dynamics in the Harmonic Approximation,* 2nd ed. (Academic, New York, 1971).

[2] J. M. Grow, D. G. Howard, R. H. Nussbaum, and M. Takeo, Phys. Rev. B 17, 15 (1978).

[3] J. W. Petersen, O. H. Nielsen, G. Weyer, E. Antoncik, and S. Damgaard, Phys. Rev. B 21, 4292 (1980); 22, 3135 (E) (1980).

[4] Yu. Kagan and Ya. A. Iosilevskii, Zh. Eksp. Teor. Fiz. 42, 259 (1962) [Sov. Phys.—JETP 15, 182 (1962)]; 44, 284 (1963) [17, 195 (1963)]; 46, 2165 (1964) [19, 1462 (1964)].

[5] R. J. Elliott and D. W. Taylor, Proc. Phys. Soc. 83, 189 (1964).

[6] P. D. Mannheim, Phys. Rev. 165, 1011 (1968), P. D. Mannheim and A. Simopoulos, 165, 845 (1968); P. D. Mannheim and S. S. Cohen, Phys. Rev. B 4, 3748 (1971); P. D. Mannheim, *ibid.* 5, 745 (1972).

[7] P. H. Dederichs and R. Zeller, *Dynamical Properties of Point Defects in Metals,* Vol. 87 of *Springer Tracts in Modern Physics,* edited by G. Höhler (Springer, Berlin, 1980).

[8] W. Cochran, CRC Crit. Rev. Solid State Sci. 2, 1 (1971).

[9] S. K. Sinha, CRC Crit. Rev. Solid State Sci. 4, 273 (1973).

[10] W. Weber, Phys. Rev. Lett. 33, 371 (1974).

[11] W. Weber, Phys. Rev. B 15, 4789 (1977).

[12] K. Kunc and O. H. Nielsen, Comput. Phys. Commun. 16, 181 (1979); 17, 413 (1979).

[13] O. H. Nielsen and W. Weber, Comput. Phys. Commun. 18, 101 (1979).

[14] J. B. Page, Jr. and B. G. Dick, Phys. Rev. 163, 910 (1967); J. B. Page, Jr. and D. Strauch, *Localized Excitations in Solids* (Plenum, New York, 1968), p. 559; Phys. Status Solidi 24, 469 (1967); D. Strauch, *ibid.* 30, 495 (1968).

[15] M. Vandevyver and D. N. Talwar, Phys. Rev. B 21, 3405 (1980); M. Vandevyver, D. N. Talwar, P. Plumelle, K. Kunc, and M. Zigone, Phys. Status Solidi B 99, 727 (1980).

[16] G. W. Lehman and R. E. DeWames, Phys. Rev. 131, 1008 (1963).

[17] H. Bilz and W. Kress, *Phonon Dispersion Relations in Insulators,* Vol. 10 of *Springer Series in Solid State*

Sciences, edited by M. Cardona, P. Fulde, and H.-J. Queisser (Springer, Berlin, 1979).
[18]D. L. Price, J. M. Rowe, and R. M. Nicklow, Phys. Rev. B 3, 1268 (1971).
[19]B. G. Dick and A. W. Overhauser, Phys. Rev. 112, 90 (1958).
[20]I. M. Lifshitz, Nuovo Cimento Suppl. 3, 716 (1956).
[21]D. N. Zubarev, Usp. Fiz. Nauk 17, 71 (1960) [Sov. Phys.—Usp. 3, 320 (1960)].
[22]R. J. Elliott, J. A. Krumhansl, and P. L. Leath, Rev. Mod. Phys. 46, 465 (1974).
[23]T. H. K. Barron, W. T. Berg, and J. A. Morrison, Proc. R. Soc. London Ser. A 242, 478 (1957).
[24]W. Ludwig, Ergeb. Exakten Naturwiss. 35, 1 (1964).
[25]R. M. Martin, Phys. Rev. 186, 871 (1969).
[26]G. Weyer, A. Nylandsted-Larsen, B. I. Deutch, J. U. Andersen, and E. Antoncik, Hyperfine Interact. 1, 93 (1975).
[27]E. Antoncik, Hyperfine Interact. 1, 329 (1976).
[28]P. C. Martin, *Ecole d'ete de Physique Theorique, Les Houches* (Gordon and Breach, London, 1967), p. 39.
[29]P. H. Dederichs, private communication.
[30]G. Gilat, Methods Comput. Phys. 15, 317 (1976).
[31]A. H. MacDonald, S. H. Vosko, and P. T. Coleridge, J. Phys. C 12, 2991 (1979).
[32]B. N. Parlett, *The Symmetric Eigenvalue Problem* (Prentice-Hall, Englewood Cliffs, 1980).
[33]S. N. Sokolev and I. N. Silin, CERNLIB routine D510, CERN report No. P810 (CERN, Geneva, Switzerland).
[34]G. Dolling, *Inelastic Scattering of Neutrons in Solids and Liquids* (IAEA, Vienna, 1963), Vol. 1, p. 37.
[35]G. Nilsson and G. Nelin, Phys. Rev. B 6, 3777 (1972).
[36]G. Nilsson and G. Nelin, Phys. Rev. B 3, 364 (1971).
[37]G. Nelin and G. Nilsson, Phys. Rev. B 5, 3151 (1972).
[38]A. S. Barker, Jr. and A. J. Sievers, Rev. Mod. Phys. 47, Suppl. No. 2 (1975).